



Contents lists available at ScienceDirect

## Saudi Journal of Biological Sciences

journal homepage: [www.sciencedirect.com](http://www.sciencedirect.com)

Original article



# How does a *Saccharomyces cerevisiae* extract influence the components of isolated rotavirus particles from stool samples collected in a clinical setting from children?

Mona A.M. Hussein<sup>a</sup>, Mayasar I. Al-zaban<sup>b</sup>, Yahia A.G. Mahmoud<sup>a</sup>, Amin A. Al-Doaiss<sup>c</sup>, Safia M.A. Bahshwan<sup>d,\*</sup>, Khalid A. El-DougDoug<sup>e</sup>, Mohamed R. EL-Shanshory<sup>f</sup>

<sup>a</sup> Botany Department, Faculty of Science, Tanta University, Tanta 31527, Egypt

<sup>b</sup> Department of Biology, College of Science, Princess Nourah bint Abdulrahman University, P.O. Box 84428, Riyadh 11671, Saudi Arabia

<sup>c</sup> Biology Department, College of Science, King Khalid University, P.O. Box 9004, Abha 61413, Saudi Arabia

<sup>d</sup> Biological Sciences Department, College of Science and Arts, King Abdulaziz University, Rabigh 21911, Saudi Arabia

<sup>e</sup> Microbiology Department, Faculty of Agriculture, Ain Shams University, PO Box 68, Hadayek Shobra 11241, Cairo, Egypt

<sup>f</sup> Pediatric Department, Faculty of Medicine, Tanta University, Tanta 31527, Egypt

## ARTICLE INFO

## Keywords:

Docking molecular  
ELISA  
Human Rotavirus  
RT-PCR  
Virus cultivation  
Yeast extract

## ABSTRACT

Human Rotavirus (HRV) is the causative pathogen of severe acute enteric infections that cause mortality among children worldwide. This study focuses on developing a new and effective treatment for rotavirus infection using an extract from *Saccharomyces cerevisiae*, aiming to make this treatment easily accessible to everyone. 15 antigens and 26 antibodies were detected in serum and stool using ELISA. The titers of HRVq1, HRVq2, HRVC1, and HRVC2 on Vero cells were determined to be  $1.2 \times 10^6$ ,  $3.0 \times 10^6$ ,  $4.2 \times 10^6$ , and  $7.5 \times 10^5$  (Plaque forming unit, PFU/ml) four days after infection, respectively. The HRVq1 isolate induced cytopathic effects, i.e., forming multinucleated, rounded, enlarged, and expanding gigantic cells. RT-PCR identified this isolate, and the accession number 2691714 was assigned to GeneBank. The molecular docking analysis revealed that nonstructural proteins (NSPs) NSP1, NSP2, NSP3, NSP4, NSP5, and NSP6 exhibited significant binding with RNA. NSP2 demonstrated the highest binding affinity and the lowest binding energy ( $-8.9$  kcal/mol). This affinity was maintained via hydrophobic interactions and hydrogen bonds spanning in length from  $1.12 \text{ \AA}$  to  $3.11 \text{ \AA}$ . The ADMET and bioactivity predictions indicated that the yeast extract possessed ideal solubility, was nontoxic, and did not cause cancer. The inhibitory constant values predicted for the *S. cerevisiae* extract in the presence of HRV vital proteins varied from  $5.32$  to  $7.45$  mM, indicating its potential as a viable drug candidate. *Saccharomyces cerevisiae* extract could be utilized as a dietary supplement to combat HRV as an alternative dietary supplement.

## 1. Introduction

Rotaviruses are responsible for subclinical enteric infections in both children and adults, with newborns being particularly vulnerable to fatal cases. Rotavirus infections can easily spread through fecal matter, as they are resistant to acidity, heat, and pH levels (Greenberg, and Estes, 2009; Ragab et al., 2024). Rotaviruses belong to the subfamily Sedoreovirinae of the Reoviridae, which is classified under the genus Rotavirus. The virus's genome comprises of a double-stranded RNA with eleven segments except for genome segmentation 11, which encodes for

a pair of proteins; each region of the genome encodes for one protein that is important for the virus lifecycle (Meyer et al., 2023).

Structural proteins comprising VP1, VP2, VP3, VP4, VP6, and VP7 are responsible for the formation of the virion and induce the generation of neutralizing antibodies, while the rotavirus-infected cell generates the following nonstructural proteins (NSPs) including NSP1, NSP2, NSP3, NSP4, NSP5, and NSP6 (Asensio-Cob et al., 2023). Badaracco et al. (2013) report that at least six of the twelve proteins listed above bind RNA NSP2, which performs crucial functions in rotavirus replication. The viral structure is icosahedral in shape, with a diameter of  $70$  nm, and

\* Corresponding author.

E-mail addresses: [Mona.amhusein@science.tanta.edu.eg](mailto:Mona.amhusein@science.tanta.edu.eg) (M.A.M. Hussein), [Mialzaban@pnu.edu.sa](mailto:Mialzaban@pnu.edu.sa) (M.I. Al-zaban), [Yehia.mahmoud@science.tanta.edu.eg](mailto:Yehia.mahmoud@science.tanta.edu.eg) (Y.A.G. Mahmoud), [aaldoaiss@kku.edu.sa](mailto:aaldoaiss@kku.edu.sa) (A.A. Al-Doaiss), [smabahashwan@kau.edu.sa](mailto:smabahashwan@kau.edu.sa) (S.M.A. Bahshwan), [Khaleel\\_ali@agr.asu.edu.eg](mailto:Khaleel_ali@agr.asu.edu.eg) (K.A. El-DougDoug), [mohamed.elshanshory@med.tanta.edu.eg](mailto:mohamed.elshanshory@med.tanta.edu.eg) (M.R. EL-Shanshory).

<https://doi.org/10.1016/j.sjbs.2024.104031>

Received 21 April 2024; Received in revised form 21 May 2024; Accepted 25 May 2024

Available online 26 May 2024

1319-562X/© 2024 The Authors. Published by Elsevier B.V. on behalf of King Saud University. This is an open access article under the CC BY-NC-ND license (<http://creativecommons.org/licenses/by-nc-nd/4.0/>).

lacks an envelope. Its capsid is formed from 3 layers: an outer, an inner capsid, & a nucleus. A total of sixty spines, ranging in length from 10 to 12 nm, emerge from the outer capsid.

Infections in various Egyptian cities including Cairo, Quliobia, Behira, Alexandria, Giza, Sharkia, & Fayoum are attributed to Rotavirus strains, with the highest prevalence observed in genotypes G1, G2, and G4 (Harb et al., 2023).

The detection of rotavirus in the laboratory is accomplished via TEM, antigen ILFSA, ELISA, & antibody ELISA. In addition, different PCR techniques are costly, yield rapid results, and possess high sensitivity. Primers that are either generic or type-specific are utilized in RT-PCR. Currently, the proteins VP4, VP6, & VP7 are the most frequently utilized ones (Gazal et al., 2011; Alkan et al., 2012; Ghonaim et al., 2023). Consequently, it constitutes a compelling subject for the evaluation of antiviral agents. Rotavirus VP4's high-resolution crystal structure was published (Alkan et al., 2012). Furthermore, their work established a framework for drug design and screening by utilizing the VP4 structure (Saady et al., 2017).

The control of the host immunity is significantly influenced by microbiota. As a result, certain clinical advisors attempt to enhance the health status of affected individuals through the administration of probiotics, which are live microbes that, when supplied in sufficient quantities, induce beneficial impacts on the host (Hoffman et al., 2008).

World Health Organization (WHO) and recent Food & Agriculture Organization (FAO) recommendations stipulate that probiotic organism used in foods must be nonpathogenic, nonpoisonous, resistant to bile salts & low pH, able to proliferate & colonize in the gut, and able to live in the gut (Wollowski et al., 2001; WHO/FAO, 2002). Even though most probiotic microorganisms found in human microbiota are lactic acid bacteria, certain strains of yeast found in dairy & fermented outcomes are considered probiotics.

Live microorganisms in the fermented foods termed probiotics and their secondary metabolites with bioactive potential were considered as potential anti-viral capabilities through various mechanisms. Given the importance of functional and fermented foods in disease prevention, there is a need to discuss the contextualization and deep understanding of the mechanism of action of these foods, particularly considering the appearance of the coronavirus (COVID-19) pandemic, which is causing health concerns and increased social services globally (Varsha et al., 2023). Probiotics such as *Saccharomyces cerevisiae*, *S. boulardii*, & certain strains of *Candida pichia* and *Kluyveromyces* are well-known due to their beneficial health impacts & antiproliferative and anti-inflammatory properties, particularly in the context of cancer. The procedures underlying these positive consequences have been the subject of research (Wollowski et al., 2001; Sergeeva et al., 2023). The mechanism of probiotic strains or their bioactive metabolites (volatile compounds, polyphenols, amino acids, and peptides) is due to the stimulation of immune response through boosting T-lymphocytes, cytokines, and cell toxicity of natural killer cells (Varsha et al., 2023; Sergeeva et al., 2023).

New drug research and development is an arduous, time-consuming endeavor that demands a substantial financial investment. Amidst the ongoing worldwide emergency, the relocation of established pharmaceuticals appears to be a possibly valuable strategy for identifying novel treatment modalities (Serafin et al., 2020). For drug discovery, computer-assisted virtual screening offers a rapid and cost-effective alternative to high-throughput screening. In addition, the selection of potential medicines can be optimized using virtual screening technology (de Carvalho Gallo et al., 2018; da Fonseca et al., 2023). Virtual screening has significantly contributed to the identification of inhibitors of small molecules of therapeutic targets over the last few decades. Small-molecule ligands for target proteins have been recognized via structure-based virtual screening techniques & a variety of ligands (Bharatham et al., 2017; Li et al., 2020).

The objective was to identify children who have been infected with a virus. Furthermore, the possible impact of probiotics (specifically *S. cerevisiae* extract) on virus composition, infection, and molecular

docking analysis will be studied to assess the inhibitory effect of yeast extract on the activity of the NSP2 protein.

## 2. Materials and methods

### 2.1. Collection & preparation of clinical blood and stools

Gloves and lab coats were worn before beginning work. All chemicals & biologic agents were disposed of parallel with local environmental & safety regulations. These procedures can be found in the following WHO (2004). This work was approved by the Faculty of Science, Tanta University Animal Testing Local Ethics Council with approval code (MAKU HADYEK-2014/12-81).

The study was done from the summer of 2022 to 2023. In total, seventy-two were selected to represent the Qalubia region (from hospitals and Special Clinical) and seventy-eight clinical blood specimen districts in Cairo, Egypt, using a confidence level (CL) of 95 % & confidence interval (CI) of 5 % & considering the approximate number of children whose acute enteric infections were reported to healthcare facilities units (Ibrahim et al., 2015). The specimens were obtained from infants, both male and female, between the ages of two and three years.

A volume of five mL containing 10 % (w/v) phosphate-buffered saline (0.01 M Tris solution, pH 7.5, 14.5 mM NaCl, & 10 mM CaCl<sub>2</sub> (Sigma, USA) was used to suspend 0.5 g of stool. The stool solution was mixed & clarified for 10 min at 3000 rpm via centrifugation (SIGMA 3-30KS, Germany). 1.5–2.0 ml of the clarified supernatant was gathered & kept at 40 °C until use.

Clinical blood samples were collected from the patient's blood vessels. Following a 10-minute centrifugation at 3,000 × g of EDTA-free blood tubes, serum samples were transported to sterile containers & preserved at 20 °C till analysis.

### 2.2. Detection of Rotavirus (HRV)

#### 2.2.1. Detection HRV antigens

Lateral flow immunoassays were applied for the Detection of HRV antigens in stool and serum in all concentrated samples by (Rotavirus MonlabTest®), (kit of CORTEZ.RapiCardInsta Test California, USA) according to Li et al. (2023).

#### 2.2.2. Enzyme-Linked immunosorbent assay (ELISA)

Using kits (C1701 RIDASCREEN® viral antigen, R-Biopharm AG, Germany), the antigens of Rotavirus were identified following the manufacturer's guidelines for qualitative Rotavirus antigen in clinical samples (Coulson and Holmes, 1984). Qualitative Rotavirus antibodies in clinical serum were identified according to Coulson and Holmes (1984).

### 2.3. Rotavirus isolation and replication in cell culture

#### 2.3.1. Cultivation of HRV

The established Vero cell line (obtained from the renal tissue of a normal African green monkey) was gained from the American Type Culture Collection (ATCC) continuous cell line (Yasumura and kawakita, 1963). Vero cells were established in Eagle's Minimum Essential Medium supplied with 0.01 % lactalbumin hydrolysate (Cecilio et al., 2012), 0.075 % sodium bicarbonate, 5 % CO<sub>2</sub>, and 5 % fresh calf serum. The culture was kept at 37 °C. The Vero cell monolayers were plated and inoculated in triplicates with cleared positive stool specimens using 100 µl of repeated serial dilutions of 10-fold (10<sup>-1</sup>–10<sup>-7</sup>). The plates were kept in humidity within an incubator with 5 % CO<sub>2</sub> & cultured for 1 to 5 days at 37 °C (Al-Ruwaili et al., 2012). After that, the supernatant was eliminated, titrated, & kept at –80 °C until needed. Uninfected monolayer in medium served as the negative control for the controls. Vero cells lyse as they pass further to reach high virus titers.

### 2.3.2. Examination of cytopathic effect (CPE)

According to Osman et al. (2015), the HRV-inoculated Vero cell plates were inspected under an inverted microscope (HUND, Germany) for development four days after injection for CPE.

### 2.3.3. Titration of virus

After removing the agarose layer, 0.1 % crystal violet solution was applied to color the plate. Plaque-forming units per milliliter, or PFU/ml, were used to assess the virus titer at the proper dilution.

### 2.3.4. Identification of Virus

**2.3.4.1. Extraction of virus particles.** After seven days of virus injection, the virus particles were isolated from infected Vero cells that were plated and displayed (cell lysis and cell death) in phosphate buffer 0.1 M, pH 7 (1:3, w: v). The Vero cells solution was centrifuged at 3000 rpm under cooling for fifteen min. The pellet was removed, & the supernatant was collected in new Eppendorf tubes.

**2.3.4.2. Extraction of virus RNA.** Viral RNA was isolated from infected Vero cells solution centrifuged at 3000 rpm under cooling for 15 min. Following the manufacturer's directions, the pellet was disposed of, & the supernatant was harvested in a fresh Eppendorf using Biozol reagent (BSC51S1, BIOFLUX, Japan).

**2.3.4.3. Determination of purity and concentrated virus.** RNA was detected by assessing the absorbance at 260 nm & purity at 260/280 nm by applying the Nanodrop (Thermo 2000C, Thermo scientific, USA). The extracted RNA for all strains was visualized using electrophoresis (Sambrook and Russel, 2001).

**2.3.4.4. Synthesis of cDNA.** Viral RNA extract (5 µl) was shocked for 5 min at 99 °C. 15 µl of a combination that includes the following ingredients: Promega, USA and Bioline, Germany provided 2 µl of five-fold RT buffer (250 mM Tris-HCl-pH 8.3), 375 mM KCl, 40 mM MgCl<sub>2</sub>, 0.08 µl of dNTPs, 0.25 µl of primer (VP7-FATGTATGGTATTGAATATACCAC), Taq DNA polymerase, reverse transcriptase from Moloney Murine Leukemia Virus, & 2.5 mM dNTP).

**2.3.4.5. Amplification of VP6 cDNA.** PCR was used to increase the cDNA. According to Ituriza-Gomara et al. (2002), one µl of cDNA was combined with 25 µl of PCR mixture (RT buffer, 375 mM KCl, 40 mM MgCl<sub>2</sub>, Taq DNA polymerase, & dNTP Mix) & 10 µl of each primer set, VP6-F 5'-AGCACAACTTTTCAGCACC-3' and VP6-R5'-GTGAAAACGCGTTGCAAGTT-3'.

**2.3.4.6. Gel analysis.** The size of the PCR product was assessed using agar gel electrophoresis compared with the DNA leader. Gels were scanned, photographed, & analyzed via the Gel Doc VILBER LOURMAT system (GmbH, Germany) (Sambrook and Russel, 2001).

**2.3.4.7. Determination of nucleotide sequence of for code HRVq1 children stool HRV isolate.** The PCR product fragment was purified utilizing a purification kit (Qiagen, Cat no: 51104). Utilizing an ABI Prism Big Dye Terminal Cycling Sequenced Ready Reaction Kit (Catalog number: 4337458, Applied biosystem, USA), sequencing was done to create a single continuous sequence (Contag). 310 DNA sequencers that are automated The VP6-DNA – HRV isolate's partial nucleotide sequence (231–802 bp) was submitted under the accession number 2691714, and the clustalw & blast programs (European Bioinformatics Institute) aligned it (Shade et al., 1986).

The partial nucleotide sequence of VP6 regain was done to determine the relation with other registered Rotavirus strains in GenBank. The sequencing was adopted from the forward direction at Macro-gen3730XL6-1518–009, Korea.

**2.3.4.8. Extraction protein and RNA of HRV HRVq1 isolate.** An Eppendorf containing 50 µl of a pre-warmed solution of 1 M Na Acetate with 1 % SDS was filled with 500 µl of HRVq1 pure HRV isolate, and the tube was incubated at 37°C for 15 min. The Eppendorf was filled with 500 µl of saturated phenol–chloroform, vortexed for one minute, & then kept at 56 °C for fifteen minutes. After one minute of vortexing, the Eppendorf were centrifuged at 14,000 rpm for five minutes. The virally coated protein, or lower phase, was moved to a new tube. A new tube was filled with the upper aqueous phase (viral nucleic acid), 3 M sodium acetate at pH 5.0 (about 40 µl), & 700 µl of ice-cold 100 % ethanol. The Eppendorf tube was incubated at –20 °C for two hours after being gently stirred by inversion four times. The Eppendorf was centrifuged at 12,000 rpm for fifteen minutes at 4 °C. To decant ethanol, the tubes were turned over onto paper and allowed to dry for more than fifteen minutes. Using a pipette, the dsRNA pellet was again placed in 30 µl of loading buffer.

The RNA concentration was detected by measuring the absorbance of 260 nm, & purification was established by measuring the absorbance of 260/280 nm. As well as protein concentration of 280 nm, & purification was assessed by measuring the absorbance & purity at 280/260 nm via the Nanodrop (Thermo 2000C, USA).

## 2.4. Preparation of probiotic

### 2.4.1. Extraction of probiotic strain

*Saccharomyces cerevisiae* extract (SE) was prepared as described by Eissa et al., (2016) as follows: *S. cerevisiae* was insulated on malt extract broth media & kept at 25 °C for four days. Cells were harvested via centrifugation at 6,000 rpm for fifteen min. The pellet was re-suspended in lyses buffer content of 50 mM K-phosphate "pH 7.0", 1 mM PMSF (Phenyl methyl sulfonyl fluoride, Sigma, USA) & 0.5 mM EDTA. Cells (10<sup>8</sup> CFU/mL) were agitated by vortex for 15 cycles for one minute with one volume of glass beads (0.5 mm) under cooling on ice for 1 min. Cell debris was removed by centrifugation at 6,000 rpm for 10 min. The pellet was rinsed with a puffer saline (40 gm/100 dist. Water) and acidified at pH 4.5 with HCl in the water path for 1 h at 65 °C. The lysate extract was sterile filtrated using 0.22 µm (Millipore-USA) and kept in the refrigerator overnight. The *S. cerevisiae* crude extract (SE) (40 gm/100 ml) was diluted in ds H<sub>2</sub>O at (10, 25, 50, 100, 200 mg/ml).

## 2.5. Characterization of SME

### 2.5.1. Detection of the bioactive compounds in SME using GC–MS analysis

500 mL of methanol containing 3 % HCl was used to soak 50 g of SE crude extract until the pH reached 1.5 (SME). *S. cerevisiae* methanol extract (SME) was heated to no more than 60 °C and concentrated under low pressure until it was dry.

The chemical composition of 0.2 g SME was dissolved in 1 mL methanol HPLC grade and then injected into GC mass performed according to Franchi et al. (1985) applying Trace GC1310-ISQ mass spectrometer (Thermo Scientific, Austin, TX, USA) with a direct capillary column TG–5MS (30 m x 0.25 mm x 0.25 µm film thickness). By comparing the components' retention durations & mass spectra to those of the WILEY 09 & NIST 11 mass spectral databases, the structures were determined.

### 2.5.2. Cytotoxicity effect of SME on Vero cells

Following Fotakis and Timbrell's, (2006) description, the maximum nontoxic concentration (MNTC) of the MTT [3-(4,5-dimethylthiazol-2-yl)-2,5-diphenyl tetrazolium bromide] was measured. A 96-well culture plate was used to generate a monolayer sheet of Vero cells. 100 µL of SME concentrations, 500,1000, 1500, 2000, 2500, 5000, and 10,000 mg /mL. The microplates were kept in an environment containing 5 % CO<sub>2</sub> and 95 % humidity for 24 h at 37 °C. They were checked often for up to two days during this time. After adding 20 µl of the 5 mg/ml stock solution to each well (Bio Basic Canada INC), the MTT solution was kept at 37 °C for 4 h. The formazan crystals were dissolved in each well using

200  $\mu$ l of acidic isopropanol (0.073 ml HCl/50 ml isopropanol). Using a spectrophotometer, the formazan solution's absorbance was determined at  $\lambda$  max 540 nm wavelength. There was a direct correlation between cell amount and optical density (OD). The plot of cytotoxicity (%) vs sample level was used in regression analysis to estimate the  $CC_{50}$  value, which was known as the level that decreased the OD of treated cells by 50 % when contrasted to the control. [Scheme 1](#)

$$\text{Cytotoxicity}(\%) = (\text{Abscontrol} - \text{Abstreatedcells}/\text{Abscontrol}) \times 100 \quad (1)$$

### 2.5.3. Determination of the effect of SME on genome and coat protein contents

To assay the effect of SME on viral protein and RNA was transferred 500  $\mu$ l of each concentrated, purified total RNA and total protein was placed into a fresh Eppendorf. An equal volume of 500  $\mu$ l was increased post adding SME to each Eppendorf tube. Each tube was vortexed for ten seconds and then incubated for fifteen minutes at 37  $^{\circ}$ C. The effect of SME on viral protein and RNA was determined via measurement of the absorbance of treated total RNA at 260 nm and treated protein at 280 nm using the Nanodrop (Thermo2000C).

### 2.5.4. Assessment of SME anti-HRV activity

**2.5.4.1. Cytopathic inhibition assay.** Viral cytopathic impact inhibition was carried out in 96-well Vero cell culture plates. After adding 50  $\mu$ L SME and 50  $\mu$ L HRV in quadruplicate to 100  $\mu$ L of Dulbecco's Modified Eagle's Medium (DMEM), the plates were kept for three days at 37  $^{\circ}$ C. Only SEM extract cells were used as controls, and Vero cells were used as the sole cell type. [Reed et al. \(1938\)](#) method was used to calculate the HRV titer (TCID<sub>50</sub>/mL). The logarithmic reduction factor (log<sub>10</sub>) of the viral count was used to calculate the SME antiviral activity about

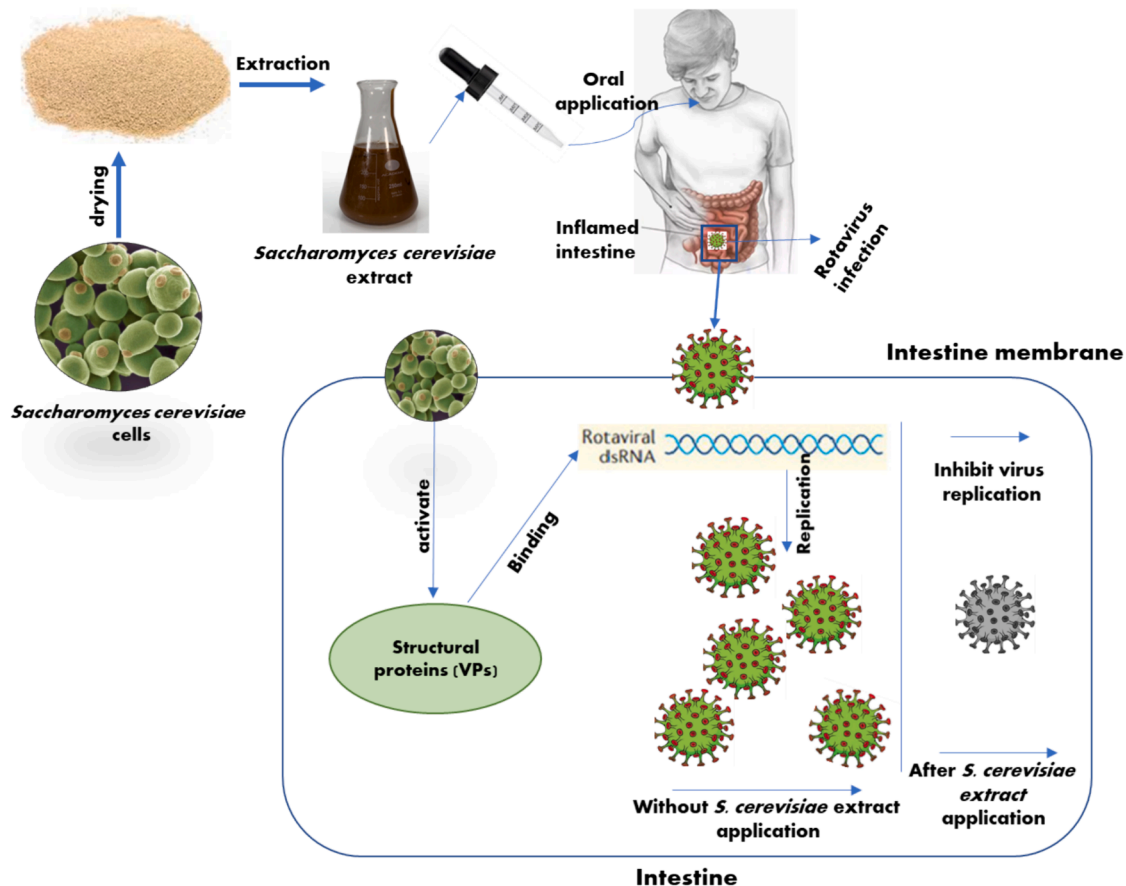
untreated infected controls. Indirect response models were used to express the results. as an inhibitory percentage (IP) and a titer (TCID<sub>50</sub>/mL), as reported by [Lelešius et al., \(2019\)](#). The subsequent formula was applied to calculate the inhibition.

$$\% \text{InhibitionPercentage}(\text{IP}) = (1 - T/C) \times 100 \quad (2)$$

Where C is the antilog of the control viral titers, and T is the antilog of the extract-treated viral titers. Positive IP was defined as equal to 98 %. The antiviral activity was first investigated by treating a single dose of MNTC versus various viral levels. According to [Kohn et al. \(2015\)](#), a 1.5 log drop in the viral titer was considered positive.

**2.5.4.2. Determination of SME anti-HRV titer.** The SME compound's action on HRV decrease was verified by the plaque test in conjunction with the IC<sub>50</sub> (50 percent inhibitory concentration) as per Hayden et al. (1980). In summary, the HRV was diluted to yield 10<sup>5</sup> PFU/well, along with 1  $\mu$ g/ml of TCPK (L-1-(tosylamido-2-phenyl) ethyl chloromethyl ketone), & the harmless levels of the evaluated SRV (2.5, 2.5, 1.25, 0.625, and 0.313  $\mu$ g/mL) on the base of the cytotoxicity assay were kept for one hour at 37  $^{\circ}$ C. After that, 100  $\mu$ l of SEM was applied to each well of a 6-well plate containing 10<sup>5</sup> Vero cells per milliliter, and the cells were allowed to adsorb the virus for one hour. After adding 3 ml of DMEM along with 2 % agarose to the Vero cell monolayer, it was kept at 37  $^{\circ}$ C until virus plaques started to develop.

After adding 10 % formalin and waiting two hours, 0.1 % safranin in distilled water was utilized to stain the plates. There were control wells where Vero cells were used to incubate the untreated virus before the number of plaques was determined. The formula used to compute the percentage decrease of plaques was viral count (untreated) – viral count (treated)/viral count (untreated) x 100. The SME level is necessary to



**Scheme 1.** Effect of *S. cerevisiae* on Rotavirus infection in children.



lower 50 % of the HRV plaque count of the viral control was named the 50 % inhibitory level (IC<sub>50</sub>). The selective index (SI) was calculated using the CC<sub>50</sub>/IC<sub>50</sub> ratio (Liu et al., 2009).

## 2.6. Molecular docking

All molecular modeling searches were achieved on a computational software basis by applying the MOLECULAR OPERATING ENVIRONMENT (MOE, 2008, USA) toward our targets as NSP 10/16 complex inhibitors and PB2 inhibitors. Each ligand-receptor complex was analyzed for binding interaction analysis, & Chimera took 3D images as visualizing software (Nafie et al., 2019).

### 2.6.1. Target selection & molecular library preparation.

One PDB code belonging to the two molecular targets for antiviral treatment procedures was selected for our study. NSP2 with function important in rotavirus replication. The PDB for the examined targets was kindly accessible via <https://www.rcsb.org/pdb/home/home.do>.

The selected target crystal structures had high resolution  $\leq 2.5$  with acceptable R-value & were conservative. In each target, water molecules & ions were observed. Moreover, hydrogens were added to the target (Taban et al., 2017). The 2-dimensional structures of GC mass-identified compounds were downloaded from the open chemistry database PubChem (<https://pubchem.ncbi.nlm.nih.gov/>). Thus, a total of 24 identified compounds, including fatty acids, esters, and steroids, were used for this study.

### 2.6.2. Molecular manipulation of the crystallographic ligands

Optimizing the Ligand chemical structure involved making adjustments to the bond order, adding charges, and introducing hydrogens. This was done using the build menu in MOLECULAR OPERATING ENVIRONMENT (MOE) software 2008. In addition, the approach of minimizing energy through conformational search or manipulating geometry was utilized (Nafie et al., 2019).

### 2.6.3. Visualization of target binding site & analysis of Ligand-Receptor interactions.

Using Chimera (Pettersen et al., 2004), we adopted a visualization of the target binding site, the disposition of the original ligand that was co-crystallized, and the main interaction between the ligand and target. This interaction was analyzed in terms of hydrogen bonding and lipophilic interaction with the key amino acid residues. The interactions were thoroughly examined based on the fundamental factors outlined in "A Medicinal Chemist's Guide to Molecular Interactions". (Bissantz et al., 2010).

## 2.7. Statistical analysis

The quantitative data were statistically based on standard deviation (SD), which was calculated as a means of three replicates. Version 23 of

the SPSS statistical program (SPSS Inc., USA) was used for all statistical computations, and Microsoft Excel 2019 was applied to form the graphs.

## 3. Results

### 3.1. Isolation and identification of Rotavirus

#### 3.1.1. HRV prevalence

Fifty clinical stool and serum samples were obtained from various institutions located in the governorates of Qalyubia and Cairo, Egypt (Table 1). HRV was diagnosed based on distanced clinical symptoms (Acute enteric severe infection, diarrhea, acute watery diarrhea, Hot, acute drought, acute holding, vomiting, Abdominal pain, Severe dehydrating diarrhea, and fever and required hospitalization). It was serologically detected in concentrated clinical stool using ILFST and ELISA tests. Principally, in young children for this study who attended hospitals, Rotavirus (HRV) antigens 42 and antibodies 62 were detected in out of 150 specimens.

Adenovirus (HAV) was detected in antigens 26, and antibodies 36 were detected in out of 150 specimens. Mixing them was detected in 7 out of 25 specimens with 7 % concentrated stool samples. Mixed 15 HAV and HRV antigens and 26 antibodies were detected in out of 150 specimens. The HRV was confirmed by biologically on Vero cell culture & RT-PCR.

#### 3.1.2. Isolation and identification

Four HRV isolates of positive clinical stool from Qalyubia (HRVq1&HRVq2) and Cairo (HRVC1 & HRVC2) distanced acute enteric severe infection were propagated on Vero cells. It appeared that the infected cells showed cytopathic effects (CPE), including the destruction, elongation, swelling, and rounding of abnormal cells. Furthermore, various sizes and morphologies of intracytoplasmic inclusions, multinucleated giant cells, and impact cells were identified. In comparison to healthy cells, the macrocytes of the infected cells endure lytic degeneration, become rounded, and acquire a fractal appearance (Fig. 1). The staining survival cells 146, 175, 154, 179 and died 54, 25, 46, 21 cells out of staining cell =  $2 \times 10^2 \mu\text{l}^{-1}$  of Vero suspension cell for HRVq1, HRVq2, HRVC1 & HRVC2 respectively (Fig. 2)

#### 3.1.3. HRV titration

The titers of the HRVq1, HRVq2, HRVC1, and HRVC2) revealed changes in shape, size, and number, and lyses Vero cell formed plaques. HRV titer was different among four children's stools were  $1.2 \times 10^6$ ,  $3.0 \times 10^6$ ,  $4.2 \times 10^6$ , and  $7.5 \times 10^5$  PFU/ml of HRVq1, HRVq2, HRVC1 & HRVC2, respectively, on Vero cell, after four days post-infection (Fig. 3).

#### 3.1.4. HRV molecular identification

**3.1.4.1. Total RNA purification.** The integrity & quantity of the purified total RNA extracted from HRV-infected Vero cells were confirmed by a

**Table 1**

HRV and HAV were serologically detected in concentrated clinical stool and serum using ILFST and ELISA tests.

Location	Clinical Specimens	Sexually	Clinical symptoms	HAV		HAV		HAV + HRV	
				ILFST	ELISA	ILFST	ELISA	ILFST	ELISA
Qalyubiyya (n = 75)	Stool (n = 50)	Girl (n = 18)	AESI, D, S	3/18	4/18	6/18	9/18	2/18	3/18
		Boy (n = 32)	AWD, H, AD,	4/32	5/32	10/32	12/32	4/32	5/32
	Serum (n = 25)	Girl (n = 12)	AH, V, AP	3/12	4/12	4/12	6/12	1/12	3/12
		Boy (n = 13)	SDD, F	2/13	4/13	4/13	7/13	2/13	3/13
Cairo (n = 75)	Stool (n = 50)	Girl (n = 10)	AESI, D, S	3/10	5/10	4/10	7/10	1/10	3/10
		Boy (n = 15)	AWD, H, AD,	3/15	6/15	5/15	8/15	1/15	3/15
	Serum (n = 25)	Girl (n = 9)	AH, V, AP	3/9	4/9	4/9	6/9	2/9	3/9
		Boy (n = 16)	SDD, F	2/16	4/16	5/16	7/16	2/16	3/16
Total n = 150				23	36	42	62	15	26

Acute enteric severe infection (AESI) diarrhea) D), acute watery diarrhea (AWD), Hot (H), acute drought (AD), acute holding (AH) vomiting(V), Abdominal pain (AP), Severe dehydrating diarrhea (SDD) and fever (F), Positive ELISA reaction was defined if the optical density (OD) of test sample exceed that of Cut off value;  $\geq 0.24$ .

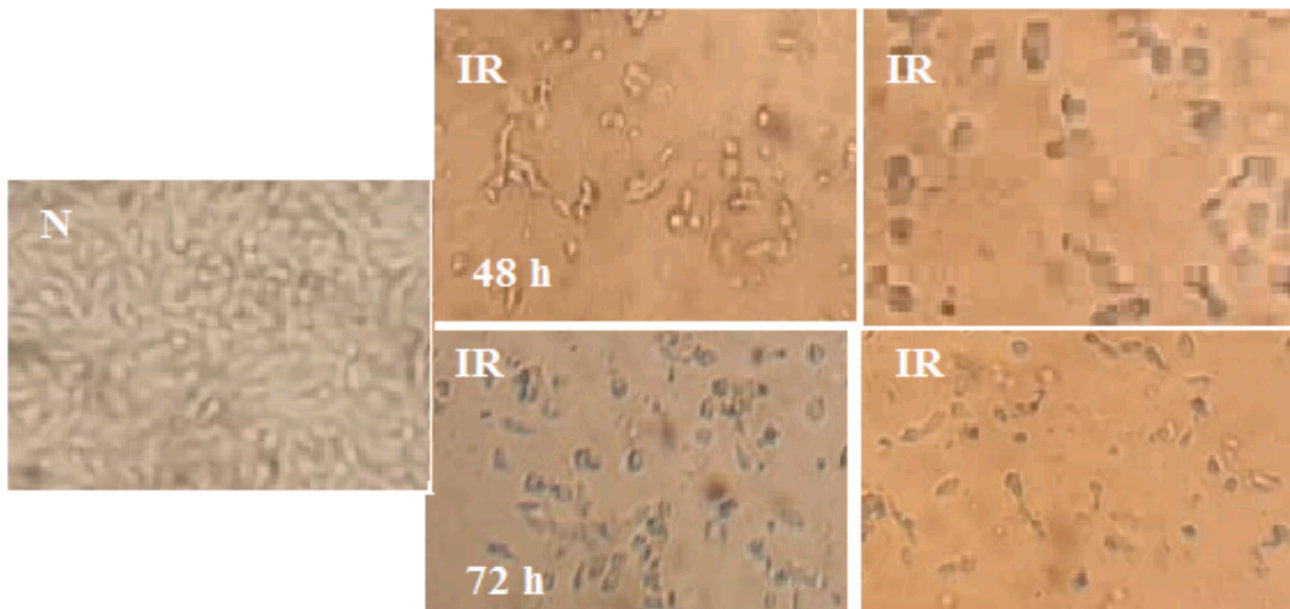


**Fig. 1.** Photo Vero cells infected with Rotavirus (IR) 48 and 72 h incubation showing Cytopathic effects as Spindle cell, swelling cell, round cell, Spinal cell and Giant cell survival cells compared normal cells (N).

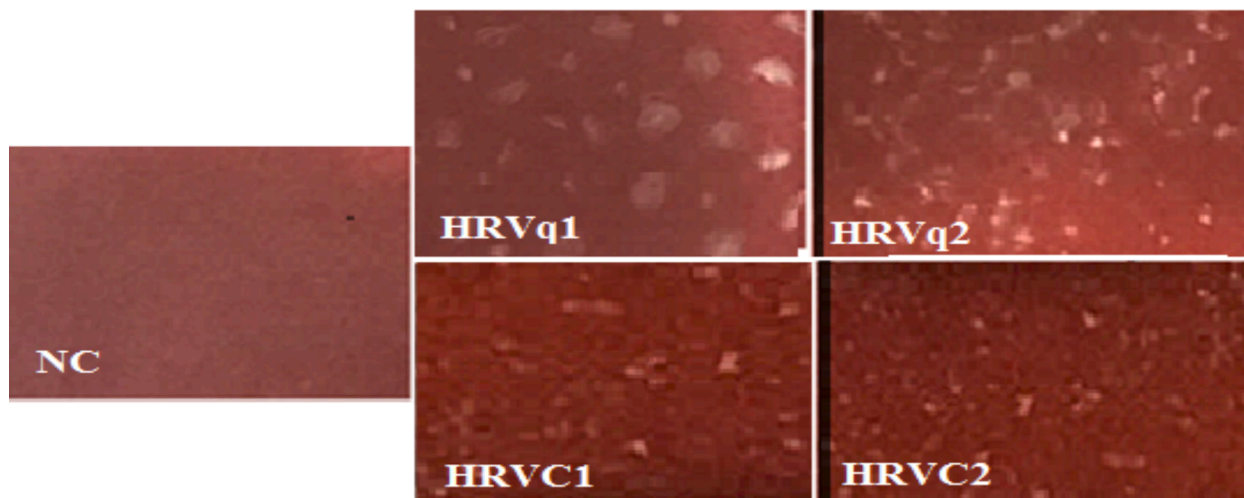


**Fig. 2.** Photo-Vero cell line Photo Vero cells infected with Rotavirus (IR) 48 and 72 h incubation showing inoculated with four HRVq1, HRVq2, HRVC1 & HRVC2 isolates showing plaques and normal cell (NC) by invert microscope.

UV spectrophotometer (Nanodrop). Using a 260/280 ratio OD, the purity level of RNAs (OD) is 1.7, 1.8, 1.9, and 2.1, respectively. The concentrations of RNA were as follows: 65, 76, 82, and 92  $\mu\text{g}/\text{mL}$  for HRVq1, HRVq2, HRVC1 & HRVC2 isolates respectively. These results indicate high yield & purity of the extracted RNAs.

**3.1.4.2. cDNA of HRV RNA VP6.** RT and a complementary primer set were utilized to transcribe the purified RNA from HRVq1, HRVq2, HRVC1, & HRVC2 into cDNA (reverse primer, VP6-R 5' GTGAAAACGCGTTGCAAGTT-3').

**3.1.4.3. VP6-R cDNA amplification.** The VP6 gene region nucleotide sequences, comprising 747 to 1126 nucleotides, were acquired for the isolates HRVq1, HRVq2, HRVC1, and HRVC2 (see Fig. 3). c DNA-VP6-R of isolates amplified by HRV using an RT-PCR reaction mix in conjunction with specific primer sets. For validating the VP6 gene amplification product, 1.5 % agarose gel electrophoresis was employed.

The size of the amplified DNA was, as anticipated, 2.00 at 550 base pairs (Fig. 3).

**3.1.4.4. Partial nucleotide sequence of VP6 gene for HRVq1 isolate.** Randomly, one positive clinical stool specimen from Qalubia (HRVq1) was used for sequence analysis. The partial PCR product of VP6 gene HRV eluted from agarose gel was purified utilizing the gel DNA extraction kit. Amplicon forming of the PCR was permitted for sequencing reaction via the automated cycle sequencing process. Sequences acquired for each primer had sufficient overlay between them & were applied to form one continuous sequence (Contag). The partial nucleotide sequence (550 bp) of vp6 gene DNA for HRV isolate was submitted  $\neq$  2691714 and done to determine the relation with other suggested isolates recorded in GenBank (Fig. 4).

### 3.2. Virus informatic analysis

The PCR-amplified fragment of VP6 of isolate HRVq1  $\neq$  2691714

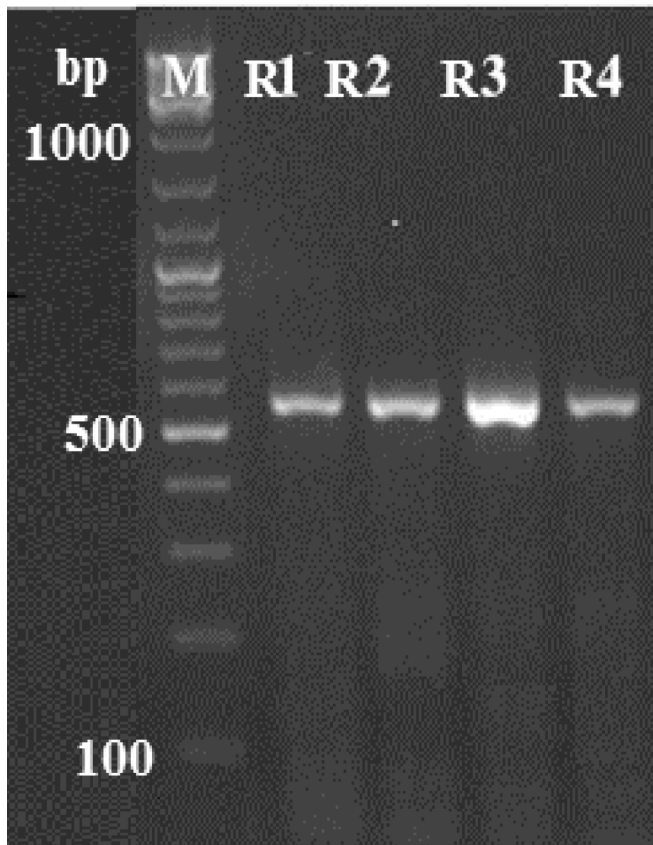


**Fig. 3.** Agarose gel (1.5 %) electrophoresis pattern of PCR products with expected size  $\approx$  550 bp from Vero cell infected with HRV using a VP6 primers (lines, (R1), HRVq1; (R2), HRVq2, (R3) HRVC1 and (R4) HRVC2). M = DNA leader molecular marker.

determined the relationship with 11 HRV isolates registered in GenBank. The sequencing and multiple alignments were adopted from the forward direction at MacroGen3730XL6-1518-009, Korea. The multiple alignments of partial nucleotide sequence VP6 gene HRV isolate  $\neq$  2691714 with 11 HRV isolates recorded in the Genbank was done using DNAMAN & MEGA.4 programmers (Wisconsin, Madison, USA). Multiple sequence alignment (MSA) was displayed Max Score ranged from 983 to 97, total score ranged from 983 to 977, Quarry Cover ranged from 100 %, E. value 00, per identity ranged from 97.73 to 97.66. Multiple sequence

alignment (MSA) was displayed in which parallel nucleotides fill the same column. The alignment of numerous genes showed the conserved sites & the % of conservation for every position. Aligned residues share the evolutionary origin & sequence resemblance to some extent.

### 3.3. Phylogenetic tree

The partial nucleotide sequence of the VP6 region of children's stool code R3 was aligned by the cluster W program with minor manual adjustments, resulting in 571 positions, involving the gaps (Fig. 5). Based on MSA analysis, the phylogenetic tree was formed & showed two clusters in which HRVq1 isolated one cluster. The second cluster included Genbank isolates into three sub-clusters that showed homologous with a genetic distance of 0.01 (Fig. 5). The nucleotide distances are about 0.01 (Fig. 4).

The genetic diversity value of all partial nucleotide sequences of the Rotavirus - VP6 population, representing the average amount of nucleotide substitutions per site among pairs of sequences, was  $0.026 \pm 0.005$ .

### 3.4. Bioactive compounds of *Saccharomyces methanol extract (SME)*

Gas chromatography-mass spectrometry (GC-MS) of SME resulted in six identified compounds, as demonstrated in Table 2. The retention time (RT) of the compounds was from 48.41 to 50.1 min. SME showed six active ingredient compounds antioxidant & antiviruses Luminol, Ethanone, Pyrrolo, Benzene methanol, Actinomycin C2, & 3,7-Diazabicyclo, which contended pyrimidine and/or purine cycles related to inhibit pathogenic viruses and bacteria, as well as for alternative to traditional antibiotics (Table 2).

### 3.5. Biological activities of SME

#### 3.5.1. The cytotoxicity effects

The MTT assay determined that the MNTC of the SEM extract on Vero cells was 5 mg/mL; in comparison to the control, this concentration did not induce any discernible alterations in cell density or morphology (Fig. 5), the 50 % cytotoxic concentration (CC50) was 417  $\mu$ g/mL.

#### 3.5.2. Antiviral activity of SME

3.5.2.1. *The HRV cytopathic inhibitory effect.* The SMEs exhibited activity against HRV, as evidenced by an inhibitory percentage (IP) of 98 %. Additionally, the SME extract's antiviral activity was initially assessed using a standard titer assay, with the MTT assay being utilized

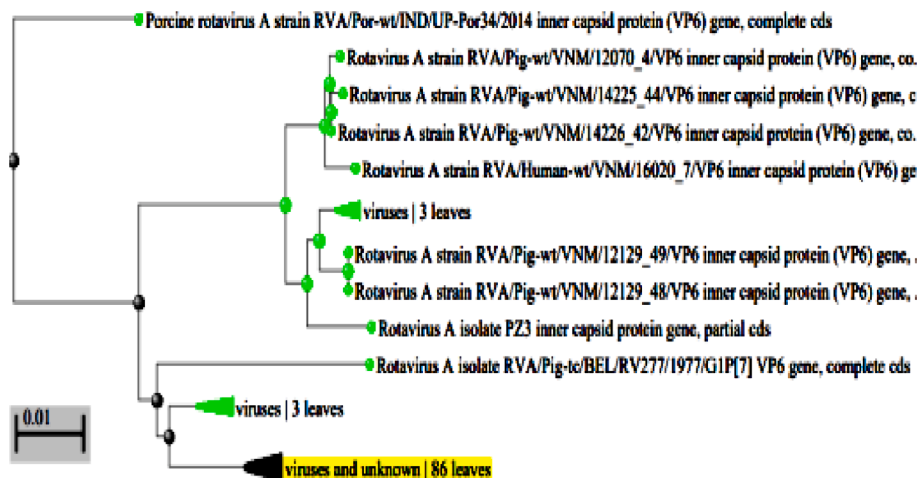


**Fig. 4.** Phylogenetic tree of partial (VP6) region nucleotide sequence of HRVq1 isolate and 9 Rotavirus isolates published in GenBank. Numbers represent bootstrap percentage values based on 1000 replicates. The genetic distance bar 0.01.



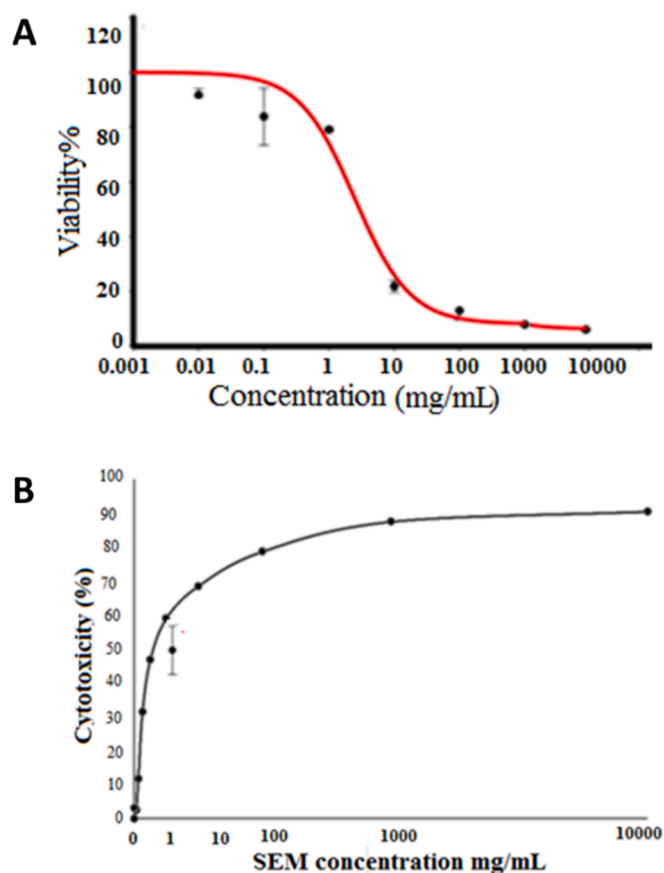


Fig. 5. Response curves of (a) Vero cell viability and (b) cytotoxicity activity of SEM extract with different concentrations for 72 h was determined by SRB stain in Vero cell assessed by MTT.

to determine the various viral concentrations. Before treatment, the viral titer resulting in 50 % cytolysis (TCID<sub>50</sub>/ml) was 104.80 (2.2 log), and it decreased to 103.25 (2.01 log) following treatment. Consequently, the MKSE extract was deemed favorable due to the 1.5 log reduction.

**3.5.2.2. The assay for plaque reduction.** The plaque-reduction test was employed to quantify the 50 % inhibitory level (EC<sub>50</sub>) and validate the compound's activity. It exhibited substantial concurrence with antiviral activity assays. The EC<sub>50</sub> and SI values for MKSE were 2.04 and 204.5 µg/mL, respectively.

Antiviral activity was observed in BRVM1-induced plaques at various safe concentrations of MKSE, with a minimal reduction of 48.89 % and a maximal reduction of 93.14 %. Plaque counts did indeed decrease significantly (Table 3).

**3.5.2.3. Effect of SME on chemical composition of HRV particles.** Protein content: Using a spectrophotometer, the HRV protein of the HRVq1 isolates isolated from children's stool appeared red at 595 nm; the protein level was assessed by applying the BSA standard curve. The protein concentration was 0.89 mg/ml.

Nucleic acid content: The quantity of nucleic acid HRVq1 isolate was ascertained using a UV spectrophotometer at a wavelength of 260 nm. The concentration was 0.65 g/ml.

**3.5.2.4. Impact of SME on chemical composition.** Impact of SME on chemical composition was denaturated treated whole particle, coat protein, and (genome)nucleic acid contents of HRV with the SME extract of somatic *Saccharomyces* cells with was denaturated HRV both of the protein and nucleic acid content of HRV particles. It is confirmed by the

change in concentration and the rate of ultraviolet absorbance (Table 4). Adjusting the protein concentration modifying from 72.543 to 54.952 mg/ml, absorb ultraviolet radiation at 280 nm from 72.54 to 54.95 nm, and purity score at 280/260 from 2.24 to 1.82 nm. The same trend result was obtained with the nuclei acid with the opposite, an increase in the concentration of the nucleic acid content from 4254.2 to 7243.5 µg/ml, an increase in the rate of UV absorbance at 260 nm from 0.52 to 0.97 nm and a purity score from 1,19 to 1.36 at 260/280 nm (Table 5).

### 3.6. Molecular modeling.

Molecular docking is widely utilized as a prominent technique within the domain of computer-aided drug development (CADD) to ascertain potential new pharmaceutical compounds. Presently, large drug libraries are annotated and analyzed rapidly using CADD, which saves an enormous quantity of time, money, and effort. The binding interactions of our target (NSP2 complex) with their co-crystallized ligands (Sinefungin) formed hydrogen bonds with amino acids. Additionally, they formed lipophilic interaction with non-polar amino acids, as shown in Table 5 and Fig. 5.

#### 3.6.1. Inhibition of HRV by SME compounds

The HRV pocket is strongly bound to SME compounds, as indicated by their binding patterns; the NSP1, NSP2, NSP3, NSP4, NSP5, & NSP6 (produced by rotavirus-infected cells) play crucial roles in rotavirus replication. The active residues exhibited robust interactions with the SME compounds Luminol, Ethanone, Pyrrolo, Benzene methanol, Diazabicyclo, and Actinomycin, as evidenced by their respective binding energies & inhibition constants of -5.6, -5.9, -7.8-6.9, -8.9, and -5.6 kcal/mol. NSP2 demonstrated the highest affinity for binding among these proteins, accompanied by the smallest binding energy of -8.9 kcal/mol. Hydrophobic interactions & hydrogen bonds spanning a range of 1.12 to 3.11 axes contributed to its stability (Fig. 6). SME compounds exhibit optimal binding to NSP2 through the formation of nine hydrogen bonds with residues. It is widely recognized that the regulation of viral transcription and replication is facilitated by the NSP2 gene located in ORF1. Additionally, many host factors have been implicated in this mechanism. Hydrophobic interaction strengthens the interaction between the SME compounds and the traditional divalent-cation binding residues.

The predicted ADMET & bioactivity appeared its best solubility, nontoxic, and non-carcinogenic features. The values of the predicted inhibitory constant of the *Sacch cerevisiae* extract with HRV vital proteins ranged from 5.32 & 7.45 mM, which proposed its promising drug candidature. This work recommended *S. cerevisiae* extract alone or in combination as a dietary supply may be applied to combat HRV after detailed *in vivo* & *in vitro* experiments.

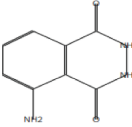
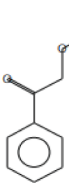
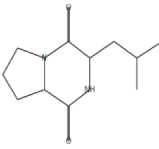
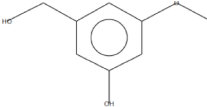
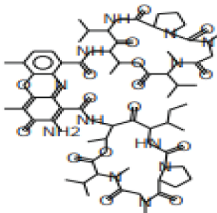
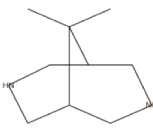
## 4. Discussion

Rotavirus disease primarily impacts children aged six years and above. Typically, the symptoms manifest themselves three days following subjection to the virus: fever, stomach upset, & vomiting for 1-3 days. Subsequently, children endure 5-8 days of watery diarrhea accompanied by a very foul odor, which precipitates rapid loss of body fluids. This is particularly hazardous for youngsters younger than two years of age (Marquardt and Freiberg, 2000).

Early detection of Rotavirus can, therefore, be achieved using rapid and sensitive techniques, i.e., lateral flow immunoassays; ELISA was critical for efficient control (Coulson and Holmes, 1984). Several prior pieces of information targeting the Rotavirus between children were adopted in various governorates in Egypt (Cairo, Quliobia, Behira, Giza, Alexandria, Sharkia, & Fayoum). Genotypes G1, G2, & G4 showed the maximum prevalence (Kamel et al., 2010; Saudy et al., 2017; Shaheen et al., 2024). Conversely, in a nearby Sharkia governorate, Hashem et al. (2012).



**Table 2**  
Identified Active ingredient compounds from *Saccharomyces* methanol extract by GC –MS.

RT	Compounds	Chemical name	Structure	M.F.& MW
50.1	Luminol	5-Amino-2,3 dihydropthalazine-1,4-dione		C <sub>8</sub> H <sub>7</sub> N <sub>3</sub> O <sub>2</sub> /177
50.1	Ethanone	2-(formyloxy)-1-phenyl		C <sub>9</sub> H <sub>8</sub> O <sub>3</sub> /164
48.41	Pyrrolo	[1,2-a] pyrazine-1,4-dione, hexahydro-3-(2-methylpropyl) Isobutylhexahydropyrrolo[1,2-a] pyrazine-1,4-dione		C <sub>11</sub> H <sub>18</sub> N <sub>2</sub> O <sub>2</sub>
48.41	Benzene methanol	3-hydroxy-5-methoxy 3-(Hydroxymethyl)-5-methoxyphenol #		C <sub>8</sub> H <sub>10</sub> O <sub>3</sub> /154
49.8	Actinomycin C2	Actinomycin D, 2A-D-alloisoleucine		C <sub>63</sub> H <sub>88</sub> N <sub>12</sub> O <sub>16</sub> / 1268
49.8	3,7-Diazabicyclo	[3.3.1] nonane, 9,9-dimethyl 9,9-Dimethyl-3,7diazabicyclo [3.3.1] nonane #		C <sub>9</sub> H <sub>18</sub> N <sub>2</sub> /154

**Table 3**  
Plaque-reduction assay with SME treatment HRV.

SME conc. mg/ml	% Plaque reduction	Log viral count PFU/mL
5	54.48 ± 1.2e	6.75 ± 0.0a
10	65.52 ± 2.1d	6.62 ± 0.1ab
100	76.31 ± 0.9c	6.45 ± 0.2b
1000	86.63 ± 2.1b	6.32 ± 0.4b
10,000	97.24 ± 2.3a	5.72 ± 0.3c

Viral plaques reduction percentages (%) represent the averages (mean ± SD) of three independent experiments compared to the untreated controls and Reduction of Log viral plaques count (PFU/ mL),

The current investigation employed immunoassays using (LFIA) to detect Rotavirus serologically in 35.72 % of samples of stool analyzed for antigens & 23.33 % of serum samples analyzed for antibodies via ELISA. The outcomes of this work are comparable to those recorded previously by [El-Senousy et al. \(2013\)](#). Furthermore, these results partially corroborate the previous study's conclusion that adenovirus does not exhibit seasonal variations (Lin et al., 2000). According to [Lin et al. \(2012\)](#), Serological examinations are exclusively useful for confirming the diagnosis of Rotavirus, as IgM antibodies were identified in cases where an earlier diagnosis was made on the fifth day following the onset of the illness. As a result, the ELISA method could be more feasible

**Table 4**  
Effect of MYE on the chemical composition of HRV particles.

Treatment	Concentration (mg/mL)	Protein 280 nm	RNA 260 nm	260/280 nm	280/260 nm
Control	72.543c	72.54	–	–	2.24
Protein (mg/ml)	MYE 54.952b	54.95	–	–	1.82
	164.176a	164.18	–	–	1.32
Nucleic acid (ug/mL)	Control 4254.2c	–	0.52	1.19	–
	MYE 7243.5b	–	0.97	1.36	–
	8926.6a	–	2.23	2.12	–

([Coulson and Holmes, 1984](#)). The WHO has specified the ELISA technique as the benchmark method for RV antigen detection in samples. Although enzyme-linked immunosorbent assays (ELISAs) provide numerical outcomes that can be accurately interpreted, they are typically not economical for testing small quantities of samples & require multiple processing steps ([Thomas et al., 1988](#)).

Production of concentrated clinical defecation in which HRV antigen was detected positively by ELISA. The cytopathic effects of these Vero cell-grown isolates were attributed to apoptosis induction ([Superti et al.,](#)

**Table 5**

Summary of ligand-receptor interactions of the co-crystallized ligand Six SME compounds binding with HRV-NSP2 protein with the receptor binding site (PBD: 4P1U).

No.	Binding energy (Kcal/mol)	No. of H- bonds	Residues	pKipred (mM)
Luminol	-5.6	3	Leu 141, Cys 145, Glu 166	6.24
Ethanone	-5.9	5	Thr 556, Tyr 619, Lys 621, Cys 622 Asp 623,	5.42
Pyrrolo	-7.8	6	Gly 163, Arg166, Glu 167, Tyr 264, Asn 267, Tyr 273,	6.75
Benzene methanol	-6.9	5	Cys391, His519, Asn544, Asp571(2),	6.54
Actinomycin C2	-8.9	6	Arg166, Glu167, Tyr264, Asn267 Asp 302 Thr 556	7.45
3,7-Diazabicyclo	-5.6	4	Tyr619, Lys621, Cys622 Asp623,,	5.32

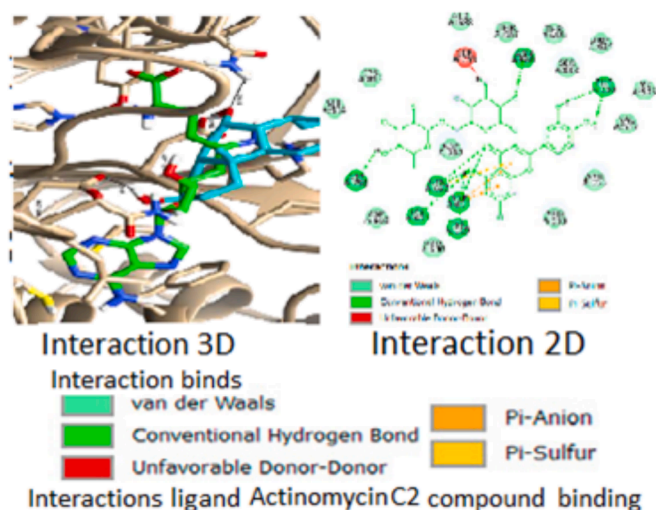


Fig. 6. 3D image of ligand-receptor interactions of the co-crystallized ligand with the receptor binding site (PDB: NSP2).

1996) and the formation of plaques of varying sizes and numbers four days post-infection (Prez et al., 2018). Our findings are consistent with those of previous research (Kittigul et al., 2001). In vitro, infection with Rotavirus was found to be linked to a range of subcellular pathological alterations, which ultimately resulted in cell lysis. The potential significance of the rotavirus-host interaction in the development of diarrheal disease has been suggested, and lytic processes have been identified as the cause of cell death (Estes, 1996).

The high purity and yield of HRVq1, HRVq2, HRVC1 & HRVC2 isolates extracted from HRV-infected Vero cells were confirmed by a UV spectrophotometer by Nanodrop. RT was utilized in conjunction with a complementary primer set for the VP6-R gene (glycoprotein and protease protein) to transcribe the purified RNA into cDNA (Trojnar et al., 2013). c DNA-VP6-R of isolates amplified by HRV using a targeted primer set and RT-PCR. Agarose gel electrophoresis was employed to validate the PCR product (El- El-Senousy et al., 2014; Osman et al., 2015). The amplified DNA exhibited the anticipated variation sizes of 774, 775, and 1126 base pairs for the HRVq1, HRVq2, HRVC1, and HRVC2 isolates, respectively.

Partial nucleotide sequence of VP6 gene for Qalubia HRVq1 isolates from purified fragment eluted from agarose gel. Amplicon forming of the PCR was permitted for sequencing reaction via the automated cycle sequencing assay. The vp6 gene DNA of isolated HRV was submitted to ≠ 2691714 GenBank and was done to determine the relationship with 11 HRV isolates registered in GenBank using DNAMAN & MEGA.4 programmers (Wisconsin, Madison, USA).

Multiple sequence alignment (MSA) was displayed. The max score ranged from 983 to 977, and the total score per identity ranged from 97.73 to 97.66 (Fong and Lipp, 2005; El-Senousy et al., 2013).

The chemical composition of HRV partials HRVq1 isolate was 0.89 mg/ml & 0.65 µg/ml with UV spectra at 595 nm and 260 nm length using the spectrophotometer for protein & RNA contents, respectively. The obtained results showed that variation in chemical composition

between the HRVq1 isolate and other HRV isolates recorded in the GeneBank (Matthijnssens et al., 2008).

GC mass of SME resulted in 12 active gradient compounds with different retention times: Luminol, Ethanone, Pyrrolo, Benzene methanol, Actinomycin C2, and 3,7-Diazabicyclo. These compounds belong to chemical antioxidants and antiviral, which contend pyrimidine and/or purine cycles related to inhibiting viruses, as well as for alternative to traditional antibiotics. These agents, formed by numerous yeast species, are also present in the inner layer of the yeast cell wall, which keeps the shape & rigidity of the cell. Mostly, these materials influence a similar composition in different yeasts, but small structural variations change principally because of their biological activity. Antioxidant activity, also, encourages apoptosis & antiproliferative impacts (Saber et al., 2017). Baker's yeast is one of the commonly utilized sources of β-glucan from *S. cerevisiae*, (Hunter et al., 2002; Shokri et al., 2008). Higher level of 5-methyltetrahydrofolate (5-CH3 H4folate) & tetrahydrofolate (H4folate) in 46 h of fermentation (Korhola et al., 2014; Saber et al., 2017). Certain strains of microorganisms, including *Saccharomyces cerevisiae*, *S. boulardii*, and *Candida pichia*, have gained recognition for their positive effects on health and their ability to inhibit cell growth and reduce inflammation, especially about cancer. The procedures that lead to these positive consequences have been extensively studied by researchers (Wollowski et al., 2001). Probiotic strains and their bioactive metabolites, such as volatile compounds, polyphenols, amino acids, and peptides, have been found to stimulate the immune response. This stimulation occurs through the boosting of T-lymphocytes, cytokines, and the cell toxicity of natural killer cells (Varsha et al., 2023; Sergeeva et al., 2023).

The exploration of alternative approaches for managing rotavirus infection is imperative due to certain challenges associated with HRV management, including the inability to eradicate the virus without causing damage to the host cells (Tomas et al., 2022). Consequently, we devised in-vitro assays utilizing both CPE inhibition and plaque decrease methods following an ethnopharmacological approach to determine the antiviral properties of SME against HRV. Vero cells were selected as the experimental subjects, and HRV was isolated from the clinical stool. This choice was based on the cells' propensity to exhibit characteristic cytotoxic & cytopathic effects, which were readily discernible through optical microscopy within a 48-hour timeframe. Furthermore, the cytotoxicity of SME was evaluated utilizing the MTT colorimetric analyze for several causes: 1) it is a straightforward procedure that can be executed on a personal computer; 2) the assessments are objective; and 3) the assessment of cytotoxicity & antiviral activity can be conducted simultaneously (Andrighetti-Frohner et al., 2005).

SME exhibited negligible cytotoxicity towards Vero cells, as evidenced by its maximum innocuous concentration (MNTC) of 5 µg/mL and CC50 value of 417 µg/mL; this had no discernible impact on the viability of Vero cells. The discrepancy in these values across studies can be attributed to the sensitivity of the cell line utilized to extract active compounds and solvents.

The SME demonstrated in-vitro antiviral capabilities against HRV in the current investigation, as evidenced by a CPE inhibitory % (IP) of 98 % and a 1.5 log lowered in HRV TCID50. Furthermore, according to the results of the plaque reduction assay, SME demonstrated EC50 values of 2.04 µg/mL & a significant SI value of 204.5. Additionally, it was

observed that the various safe concentrations of SME exhibited antiviral activity in inhibiting HRV-induced plaques, with a minimum decrease of 48.89 % at a level of 0.313  $\mu\text{g}/\text{mL}$  & highest decrease of 93.14 % at 5  $\mu\text{g}/\text{mL}$ . This trend was consistent with the observation that the number of rotavirus plaques decreased as the SME level increased.

The information mentioned earlier provides further support for the anti-rotavirus activity of *S. cerevisiae* methanol extract (SME), which inhibits viral replication directly and does not induce cytotoxicity. The antiviral activity observed in the SME may be ascribed to the active constituents Luminol, Ethanone, Pyrrolo, Benzene methanol, Actinomycin C2, & 3,7-Diazabicyclo, as identified by GC-mass analysis (Vanachayangkul et al., 2011).

Despite the considerable amount of research dedicated to the identification and separation of bioactive molecules, it is important to acknowledge the intricate nature of plants and the possibility that the observed activity is due to a synergistic interaction of chemicals (van Vuuren, 2008). Several plant extracts may inhibit Rotavirus; however, additional research is required to identify the most effective plants & determine their mechanisms of action.

The MTT test was used to determine the cytotoxicity of the SEM extract. The results indicated that the MNTC of the extract on Vero cells was 5  $\mu\text{g}/\text{mL}$ , which failed to induce any observable alterations in cell density or morphology when contrasted to the control. Furthermore, 417  $\mu\text{g}/\text{mL}$  was the 50 % cytotoxic concentration (CC50).

The impact of SME on the chemical composition of HRV particles led to denaturation in both the protein and nucleic acid. It is confirmed by the change in concentration and the rate of ultraviolet absorbance. Adjusting the concentration in the protein content in the virus particle was modified from 72.543 to 54.952  $\text{mg}/\text{mL}$  absorb ultraviolet radiation at a wavelength of 280 nm from 72.54 to 54.95 nm.

The same trend result was obtained with the nucleic acid with the opposite, an increase in the concentration of the nucleic acid content from 4254.2 to 7243.5  $\mu\text{g}/\text{mL}$ , as well as an increase in the rate of ultraviolet absorbance in nucleic acid content at 260 nm from 0.52 to 0.97 wavelength and a purity score from 1.19 to 1.36 at 260/280 nm. Currently, it has been appropriate that the metabolism of dietary materials by host gut microbiome may release some mutagenic substances such as diacylglycerols, fecapentaenes, sulfide, secondary bile acids, & reactive oxygen species that cause DNA destruction (Candela et al., 2011).

Molecular docking is widely utilized as a prominent technique within the domain of computer-aided drug development (CADD) to ascertain potential new pharmaceutical compounds. Presently, large drug libraries are annotated and analyzed rapidly using CADD, which saves an enormous quantity of time, money, and effort. NSP2 HRV Complex.

The binding interactions of our target (NSP2 complex) with their co-crystallized ligands (Sinefungin) formed hydrogen bonds with Asn 43, Asp 99, Leu 100, Cys 115, and Asp 130 as a key amino acid. Additionally, they formed lipophilic interaction with non-polar amino acids. One of the most widely used techniques in CADD for the recognition of novel medicine leads is molecular docking (Hughes et al., 2011).

In the current era, CADD is being used to annotate & analyze big medicine libraries at once, hence saving a massive amount of energy, time, & costs (Chen et al., 2016). Molecular docking is used to detect SME as a potentially active phytochemical against HRV NSP1, NSP2, NSP3, NSP4, NSP5 & NSP6. The schematic depiction of the genomic arrangement of HRV reveals that it inhibits structural proteins and nonstructural proteins, including NSP1 (Papain-like protease), NSP2 (3c-like protease), and NSP1. An examination was conducted on the most important residues of the binding site and the mechanism of inhibition by analyzing a variety of published articles and available crystal structures.

Grid frames of appropriate dimensions were utilized to enclose the active sites surrounding the crystalline shapes of HRV NSP1, NSP2, NSP3, NSP4, NSP5, & NSP6. The binding energies of HRV have been established to be -7.6, -8.9, -7.8-8.9, -9.9, & -7.6 kcal/mol,

respectively, based on its binding affinity. Comparing and studying the binding affinity of various compounds/ligands with their specific target molecule requires the binding energy (Kcal/mol); thus, the ligand's affinity for the receptor increases as its binding energy decreases. Consequently, for further research, the ligand with the greatest affinity may be selected as a probable medicine (Hopkins et al., 2014).

The intense binding observed in the domain of HRV VP6 genes by the compounds described in Choi et al. (2015) study indicates that they may be capable of inducing a substantial inhibition of the HRV VP6 gene. The optimal binding of SME compounds to VP6 is achieved via the formation of nine hydrogen bonds with residues. It is widely recognized that the VP6 gene, which is in ORF1ab, regulates viral replication and transcription. Additionally, several host factors have been implicated in this mechanism. VP6 is a cofactor in the synthesis of virus RNA, which is facilitated by the VP6 gene. Like other polymerases, the HRV VP6 domain's active site is composed of conserved motifs A through G located in the palm domain. By way of a groove secured by motifs F and G, the RNA template is assumed to enter the active site, which is comprised of motifs A & C (Gao et al., 2020).

The combination of SME compounds interacts powerfully with the residues. The hydrophobic interaction between the SME compounds and the traditional divalent-cation-binding residues strengthens the interaction. The active residues exhibit a robust interaction with the SME compounds Luminol, Ethanone, Pyrrolo, Benzene methanol, Diazabicyclo, and Actinomycin, with respective binding energies & inhibition constants of -5.6, -5.9, -7.8-8.9, -5.9, & -7.6 kcal/mol.

As structural proteins comprise virions. The cell that has been infected with Rotavirus generates the following nonstructural proteins. 6 out of the 12 proteins enumerated above bind RNA. Among these, NSP2 is particularly significant in the life cycle of Rotavirus, and its absence from individuals renders these viral proteins desirable targets for enhancing anti-rotavirus drugs. Flavonoids comprise over 9000 compounds, making them one of the most extensive classes of specialized metabolites (Yonekura-Sakakibara et al., 2019; Srivastava et al., 2023).

It was determined that these possess antimicrobial and antiviral properties. To impede the spread of viruses, they obstruct the entry of viruses into cells or disrupt the various phases of viral replication, transcription, and translation (Choi et al., 2015). The inhibitory impacts of multiple flavonoids on specific targets of the MERS and SARS coronaviruses have been recognized (da Fonseca et al., 2023).

One of the medically significant flavonoids, ethanol and actinomycin, are flavonoids that are abundant in many plants, including buckwheat, apples, tea, cherries, apricots, grapes, and oranges. They are a well-known natural antioxidant (Lin et al., 2012). Anti-inflammatory, vasoactive, antiplatelet, antiallergic, antihypertensive, antispasmodic, hypolipidemic, cytoprotective, antiprotozoal, anticancer, antiviral & antibacterial are some of the pharmaceutical properties associated with *S. cerevisiae* (Patel and Patel, 2019). Additionally, it was discovered that *Saccharomyces cerevisiae* reduced the pathogenicity of enteroviruses (Lin et al., 2012).

The precise mechanism by which viral burden is decreased remains obscure. Additionally, it was documented to impede a wide spectrum of viral proteases, including enteroviral protease (Choi et al., 2015), human norovirus protease (Jo et al., 2020). Using in silico procedures, we investigated the function of rutin in inhibiting the entry, replication, and spread of SARS-CoV-2 via the Mpro, PLpro, RdRp, and S proteins. This research was conducted to combat the COVID-19 pandemic.

## 5. Conclusions

Recent research has revealed that Rotavirus is present in edible food products in Egypt. This discovery highlights the significant health hazard it poses, especially to young children. The government must take immediate and effective action to prevent and control the spread of this viral infection. Based on the initial results of the study, the yeast extract



could have promising properties as a natural antiviral agent against Rotavirus. Further research is needed to understand the antiviral activity of yeast fully. This will involve conducting in-vivo experiments to identify the active compound and assess its clinical significance and potential mode of action in animal models of infection.

### CRedit authorship contribution statement

**Mona A.M. Hussein:** Resources, Investigation, Formal analysis. **Mayasar I. Al-zaban:** Writing – review & editing, Methodology. **Yahia A.G. Mahmoud:** Methodology, Data curation, Conceptualization. **Amin A. Al-Doaiss:** Resources, Methodology, Data curation. **Safia M.A. Bahshwan:** Writing – original draft, Methodology, Investigation. **Khalid A. El-Dougoud:** Writing – original draft, Supervision, Methodology. **Mohamed R. EL-Shanshory:** Writing – review & editing, Supervision, Data curation.

### Declaration of Competing Interest

The authors declare that they have no known competing financial interests or personal relationships that could have appeared to influence the work reported in this paper.

### Acknowledgments

The authors gratefully acknowledge Princess Nourah bint Abdulrahman University Researchers Supporting Project number (PNURSP2024R84), Princess Nourah bint Abdulrahman University, Riyadh, Saudi Arabia. The authors extend their appreciation to the Deanship of Scientific Research at King Khalid University for supporting this work through large groups under grant number (R.G.P. 2/11/44).

### References

- Alkan, F., Gulyaz, V., Timurkan, M.O., Iyisan, S., Ozdemir, S., Turan, N., 2012. A large outbreak of enteritis in goat flocks in Marmara, Turkey, by G8P group A rotaviruses. *Arch. Virol.* 157, 1183–1187. <https://doi.org/10.1007/s00705-012-1263-5>.
- Al-Ruwaili, M.A., Khalil, O.M., Selim, S.A., 2012. Viral and bacterial infections associated with camel (*Camelus dromedarius*) calf diarrhea in North Province, Saudi Arabia. *Saudi J. Biol. Sci.* 19 (1), 35–41. <https://doi.org/10.1016/j.sjbs.2011.10.001>.
- Andrihetti-Fröhner, C., Sincero, T.C.M., Da Silva, A.C., Savi, L.A., Gaido, C.M., Bettega, J.M.R., Simões, C.M.O., 2005. Antiviral evaluation of plants from Brazilian atlantic tropical forest. *Fitoterapia* 76 (3–4), 374–378. <https://doi.org/10.1016/j.fitote.2005.03.010>.
- Asensio-Cob, D., Rodríguez, J.M., Luque, D., 2023. Rotavirus particle disassembly and assembly in vivo and in vitro. *Viruses* 15 (8), 1750. <https://doi.org/10.3390/v15081750>.
- Badaracco, A., Garaicoechea, L., Matthijssens, J., Louge Uriarte Odeon, A., Bilbao, G., Fernandez, F., Parra, G.I. and Parreno, V., 2013. Phylogenetic analyses of typical bovine Rotavirus genotypes G6, G10, P and P circulating in Argentinean beef and dairy herds. *Infect. Genet. Evol.* 18, 18–30. DOI: 10.1016/j.meegid.2013.04.023.
- Bharatham, N., Finch, K.E., Min, J., Mayasundari, A., Dyer, M.A., Guy, R.K., Bashford, D., 2017. Performance of a docking/molecular dynamics protocol for virtual screening of nutlin-class inhibitors of Mdmx. *J. Mol. Graph. Model.* 74, 54–60. <https://doi.org/10.1016/j.jmgl.2017.02.014>.
- Candela, M., Guidotti, M., Fabbri, A., Brigidi, P., Franceschi, C., Fiorentini, C., 2011. Human intestinal microbiota: cross-talk with the host and its potential role in colorectal cancer. *Crit. Rev. Microbiol.* 37 (1), 1–14. <https://doi.org/10.3109/1040841X.2010.501760>.
- Cecilio, A.B., de Faria, D.B., de Carvalho Oliveira, P., Caldas, S., de Oliveira, D.A., Sobral, M.E.G., de Almeida, V.L., 2012. Screening of Brazilian medicinal plants for antiviral activity against rotavirus. *J. Ethnopharmacol.* 141 (3), 975–981. <https://doi.org/10.1016/j.jep.2012.03.031>.
- Chen, D., Oezguen, N., Urvil, P., Ferguson, C., Dann, S.M., Savidge, T.C., 2016. Regulation of protein-ligand binding affinity by hydrogen bond pairing. *Sci. Adv.* 2 (3), e1501240.
- Choi, J.H., Kim, D.W., Park, S.E., Lee, H.J., Kim, K.M., Kim, K.J., Kim, S., 2015. Anti-thrombotic effect of rutin isolated from *Dendropanax moribifera* Leveille. *J. Biosci. Bioeng.* 120 (2), 181–186. <https://doi.org/10.1016/j.jbiosc.2014.12.012>.
- Coulson, B.S., Holmes, I.H., 1984. An improved enzyme-linked immunosorbent assay for the detection of rotavirus in faeces of neonates. *J. Virol. Methods* 8, 165–179. [https://doi.org/10.1016/0166-0934\(84\)90011-9](https://doi.org/10.1016/0166-0934(84)90011-9).
- da Fonseca, A.M., Caluaco, B.J., Madureira, J.M.C., Cabongo, S.Q., Gaieta, E.M., Djata, F., Marinho, E.S., 2023. Screening of potential inhibitors targeting the main protease structure of SARS-CoV-2 via molecular docking, and approach with molecular dynamics, RMSD, RMSF, H-bond, SASA and MMGBSA. *Mol. Biotechnol.* 55, 1–15. <https://doi.org/10.1007/s12033-023-00831-x>.
- de Carvalho Gallo, J.C., de Mattos Oliveira, L., Araújo, J.S.C., Santana, I.B., dos Santos Junior, M.C., 2018. Virtual screening to identify *Leishmania braziliensis* N-myristoyltransferase inhibitors: pharmacophore models, docking, and molecular dynamics. *J. Mol. Model.* 24, 1–10. <https://doi.org/10.1007/s00894-018-3791-8>.
- El-Senousy, W.M., Barakat, A.B., Ghanem, H.E., Kamel, M.A., 2013. Molecular epidemiology of human adenoviruses and rotaviruses as candidate viral indicators in the Egyptian sewage and water samples. *World Appl. Sci. J.* 27 (10), 1235–1247. <https://doi.org/10.5829/idosi.wasj.2013.27.10.81200>.
- El-Senousy, W.M., El-Gamal, M.S., Mousa, A.A., El-Hawary, S.E., Fathi, M.N., 2014. Prevalence of noroviruses among detected enteric viruses in Egyptian aquatic environment. *World Appl. Sci. J.* 32 (11), 2186–2205. <https://doi.org/10.5829/idosi.wasj.2014.32.11.91108>.
- Estes, M.K., 2001. Rotavirus and their replication. In: Knipe, D.M., Howley, P.M. (Eds.), *Fields Virology*, 4th Ed. Lippincott Williams and Wilkins, Philadelphia; PA, pp. 1747–1785.
- Fong, T.T., Lipp, K.E., 2005. Enteric viruses of humans and animals in aquatic environments: Health risks, detection, and potential water quality assessment tools. *Microbiol. Mol. Biol. Rev.* 69 (2), 357–371. <https://doi.org/10.1128/MMBR.69.2.357-371.2005>.
- Fotakis, G., Timbrell, J.A., 2006. *In vitro* cytotoxicity assays: comparison of LDH, neutral red, MTT and protein assay in hepatoma cell lines following exposure to cadmium chloride. *Toxicol. Lett.* 160 (2), 171–177. <https://doi.org/10.1016/j.toxlet.2005.07.001>.
- Franchi, G.G., Bovalini, L., Martelli, P., Ferri, S., Sbardellati, E., 1985. High performance liquid chromatography analysis of the furanochromones khellin and visnagin in various organs of *Ammi visnaga* (L.) Lam. at different developmental stages. *J. Ethnopharmacol.* 14 (2–3), 203–212. [https://doi.org/10.1016/0378-8741\(85\)90088-1](https://doi.org/10.1016/0378-8741(85)90088-1).
- Gao, Y., Yan, L., Huang, Y., Liu, F., Zhao, Y., Cao, L., Rao, Z., 2020. Structure of the RNA-dependent RNA polymerase from COVID-19 virus. *Science* 368 (6492), 779–782. <https://doi.org/10.1126/science.abb7498>.
- Gazal, S., Taku, A.K., Kumar, B., 2011. Predominance of rotavirus genotype G6P [11] in diarrhoeic lambs. *Vet. J.* 193, 299–300. <https://doi.org/10.1016/j.tvjl.2011.11.018>.
- Ghonaim, A.H., Hopo, M.G., Ghonaim, N.H., Jiang, Y., He, Q., Li, W., 2023. The epidemiology of circulating rotavirus associated with diarrhea in Egyptian kids and calves: A Review. *Zoonoses* 3 (1), 3–15. <https://doi.org/10.15212/ZOONOSES-2023-0004>.
- Greenberg, H.B., Estes, M.K., 2009. Rotaviruses: from pathogenesis to vaccination. *Gastroenterology* 136 (6), 1939–1951. <https://doi.org/10.1053/j.gastro.2009.02.076>.
- Harb, N., Sarhan, A.G., El Dougdoud, K.A., Gomaa, H.H., 2023. *Ammi-visnaga* extract; a novel phyto-antiviral agent against bovine rotavirus. *Virus Dis.* 34 (1), 76–87. <https://doi.org/10.1007/s13337-022-00803-w>.
- Hashem, S., Shoman, S.A., Mohamed, A.F., 2012. Isolation and molecular genotyping of group A rotavirus strains circulating among Egyptian infants and children. *Egypt. J. Med. Microbiol.* 21 (3), 11–20. <https://doi.org/10.12816/0004888>.
- Hoffman, F.A., Heimbach, J.T., Sanders, M.E., Hibberd, P.L., 2008. Executive summary: scientific and regulatory challenges of development of probiotics as foods and drugs. *Clin. Infect. Dis.* 46 (Supplement 2), S53–S57. <https://doi.org/10.1086/523342>.
- Hopkins, A. L., Keserü, G. M., Leeson, P. D., Rees, D. C., Reynolds, C. H., 2014. The role of ligand efficiency metrics in drug discovery. *Nat. Rev. Drug Discov.* 13(2), 105–121. DOI: 10.1038/nrd4163.
- Hughes, J.P., Rees, S., Kalindjian, S.B., Philpott, K.L., 2011. Principles of early drug discovery. *Br. J. Pharmacol.* 162 (6), 1239–1249. <https://doi.org/10.1111/j.1476-5381.2010.01127.x>.
- Hunter, K., Gault, R., Berner, M., 2002. Preparation of microparticulate beta-glucan from *Saccharomyces cerevisiae* for use in immune potentiation. *Let. Appl. Microbiol.* 35, 267–271. <https://doi.org/10.1046/j.1472-765x.2002.01201.x>.
- Ibrahim, S.B., El-Bialy, A.A., Mohammed, M.S., El-Sheikh, A.O., Elhewala, A., Bahgat, S., 2015. Detection of Rotavirus in children with acute gastroenteritis in zagazig university hospitals in Egypt. *Electron. Physician* 7 (5), 1227. <https://doi.org/10.14661/1227>.
- Jo, S., Kim, S., Shin, D.H., Kim, M.S., 2020. Inhibition of SARS-CoV 3CL protease by flavonoids. *J. Enzyme Inhib. Med. Chem.* 35 (1), 145–151. <https://doi.org/10.1080/14756366.2019.1690480>.
- Kamel, A.H., Ali, M.A., El-Nady, H.G., Aho, S., Pothier, P., Belliot, G., 2010. Evidence of the co-circulation of enteric viruses in sewage and in the population of Greater Cairo. *J. Appl. Microbiol.* 108 (5), 1620–1629. <https://doi.org/10.1111/j.1365-2672.2009.04562.x>.
- Kittigul, L., Khamoun, P., Sujjarat, D., Utrarachkij, F., Chitpirom, K., Chaichantanakit, N., Vathanophas, K., 2001. An improved method for concentrating rotavirus from water samples. *Mem. Inst. Oswaldo. Cruz.* 96, 815–821. <https://doi.org/10.1590/s0074-02762001000600013>.
- Kohn, L.K., Foglio, M.A., Rodrigues, R.A., Sousa, I.D.O., Martini, M.C., Padilla, M.A., Arns, C.W., 2015. *In-vitro* antiviral activities of extracts of plants of the *Brazilian cerrado* against the avian metapneumovirus (aMPV). *Brazilian J. Poul. Sci.* 17, 275–280. <https://doi.org/10.1590/1516-635x1703275-280>.
- Korhola, M., Hakonen, R., Juuti, K., Edelmann, M., Kariluoto, S., Nyström, L., Piironen, V., 2014. Production of folate in oat bran fermentation by yeasts isolated from barley and diverse foods. *J. Appl. Microbiol.* 117 (3), 679–689. <https://doi.org/10.1111/jam.12564>.
- Lelešius, R., Karpovaitė, A., Mickienė, R., Drevinskas, T., Tiso, N., Ražaiškienė, O., Šalomska, A., 2019. *In vitro* antiviral activity of fifteen plant extracts against avian

- infectious bronchitis virus. BMC Vet. Res. 15, 1–10. <https://doi.org/10.1186/s12917-019-1925-6>.
- Li, G., Li, Q., Wang, X., Liu, X., Zhang, Y., Li, R., Zhang, G., 2023. Lateral flow immunoassays for antigens, antibodies and haptens detection. Int. J. Biol. Macromol. 242 (4), 125186 <https://doi.org/10.1016/j.ijbiomac.2023.125186>.
- Li, T., Tan, X., Yang, R., Miao, Y., Zhang, M., Xi, Y., Li, B., 2020. Discovery of novel glyceraldehyde-3-phosphate dehydrogenase inhibitor via docking-based virtual screening. Bioorg. Chem. 96, 103620 <https://doi.org/10.1016/j.bioorg.2020.103620>.
- Lin, Y.J., Chang, Y.C., Hsiao, N.W., Hsieh, J.L., Wang, C.Y., Kung, S.H., Lin, C.W., 2012. Fisetin and rutin as 3 protease inhibitors of enterovirus A71. J. Virol Methods 182 (1–2), 93–98. <https://doi.org/10.1016/j.jviromet.2012.03.020>.
- Liu, A.L., Shu, S.H., Qin, H.L., Lee, S.M.Y., Wang, Y.T., Du, G.H., 2009. *In vitro* anti-influenza viral activities of constituents from *Caesalpinia sappan*. Planta Medica 75 (04), 337–339. <https://doi.org/10.1055/s-0028-1112208>.
- Marquardt, O., Freiberg, B., 2000. Antigenic variation among foot-and-mouth disease virus type A field isolates of 1997–1999 from Iran. Vet. Microbiol. 74 (4), 377–386. [https://doi.org/10.1016/S0378-1135\(00\)00194-2](https://doi.org/10.1016/S0378-1135(00)00194-2).
- Meyer, A., Mazzara, C., Lava, S.A.G., Treglia, G., Bianchetti, M.G., Goeggel Simonetti, B., Simonetti, G.D., 2023. Neurological complications of rotavirus infection in children: A systematic review and meta-analysis. Acta Paediatrica 112 (7), 1565–1573. <https://doi.org/10.1111/apa.16775>.
- Nafie, M.S., Tantawy, M.A., Elmgied, G.A., 2019. Screening of different drug design tools to predict the mode of action of steroidal derivatives as anti-cancer agents. Steroids 152, 108485. <https://doi.org/10.1016/j.steroids.2019.108485>.
- Osman, Y.A., El-Senousy, W.M., El-Morsi, A.A., Rashed, M.K., 2015. Efficiency of traditional water treatment plant and compact units in removing viruses. Int. J. Appl. Sci. Biotechnol. 3 (3), 528–536. <https://doi.org/10.3126/ijasbt.v3i3.13332>.
- Patel, K., Patel, D.K., 2019. The beneficial role of rutin, a naturally occurring flavonoid in health promotion and disease prevention: A systematic review and update. In: Bioactive Food as Dietary Interventions for Arthritis and Related Inflammatory Diseases. Elsevier, p. 457e479. <https://doi.org/10.1016/B978-0-12-813820-5.00026-X>.
- Petersen, E.F., Goddard, T.D., Huang, C.C., Couch, G.S., Greenblatt, D.M., Meng, E.C., Ferrin, T.E., 2004. UCSF Chimera—a visualization system for exploratory research and analysis. J. Comput. Chem. 25, 1605–1612. <https://doi.org/10.1002/jcc.20084>.
- Prez, V.E., Martínez, L.C., Victoria, M., Giordano, M.O., Masachessi, G., Ré, V.E., Nates, S.V., 2018. Tracking enteric viruses in green vegetables from central Argentina: potential association with viral contamination of irrigation waters. Sci. Total Environ. 637, 665–671. <https://doi.org/10.1016/j.scitotenv.2018.05.044>.
- Ragab, A. S., Hmed, A. A., Sofy, A. R., 2024. Survival factors affecting the infectivity of hepatitis A virus isolated from Egypt. Microbes Infect. Dis.5(1), 113-126. 10.21608/mid.2023.237037.1619.
- Reed, L.J., Muench, H., Ajoe, J., 1938. A simple method of estimating fifty percent endpoints. Am. J. Epidemiol. 27 (3), 493–497. <https://doi.org/10.1093/oxfordjournals.aje.a118408>.
- Saber, A., Alipour, B., Faghfoori, Z., Yari Khosroushahi, A., 2017. Cellular and molecular effects of yeast probiotics on cancer. Crit. Rev. Microbiol. 43 (1), 96–115. <https://doi.org/10.1080/1040841X.2016.1179622>.
- Sambrook, J., and Russell, D.W., 2001. Molecular Cloning: A laboratory manual, Cold Spring Harbor Laboratory Press, New York, USA 1, 112–118.
- Saudy, N., Elshabrawy, W.O., Megahed, A., Foad, M.F., Mohamed, A.F., 2017. Genotyping and clinic epidemiological characterization of rotavirus acute gastroenteritis in Egyptian children. Pol. J. Microbiol. 65 (4), 433–442. <https://doi.org/10.5604/17331331.1227669>.
- Serafin, M.B., Bottega, A., Foletto, V.S., da Rosa, T.F., Hörner, A., Hörner, R., 2020. Drug repositioning is an alternative for the treatment of coronavirus Covid-19. Int. J. Antimicrob. Agents 55 (6), 105969. <https://doi.org/10.1016/j.ijantimicag.2020.105969>.
- Sergeeva, I., Permyakova, L., Markov, A., Ryabokoneva, L., Atuchin, V., Anshukov, A., Proskuryakova, L., 2023. Peptides of yeast *Saccharomyces cerevisiae* activated by the aquatic extract of *Atriplex sibirica* L. ACS Food Sci Technol. 4 (1), 173–189. <https://doi.org/10.1021/acsfoodscitech.3c00455>.
- Shade, R.O., Blundell, M.C., Cotmore, S.F., Tattersall, P., Astell, C.R., 1986. Nucleotide sequence and genome organization of human parvovirus B19 isolated from the serum of a child during aplastic crisis. J. Virol. 58 (3), 921–936. <https://doi.org/10.1128/JVI.58.3.921-936.1986>.
- Shaheen, M.N., Abd Al-Daim, S.E., Ahmed, N.I., Khalifa, M.K., Seif, W.H., Ahmed, S.S., Khairy, W.M., 2024. Prevalence and molecular characterization of rotavirus strains circulating among children with gastroenteritis in Egypt. Egypt. Pharm. J. 23 (2), 223–236. <https://doi.org/10.4103/epj.epj.326.23>.
- Shokri, H., Asadi, F., Khosravi, A.R., 2008. Isolation of beta-glucan from the cell wall of *Saccharomyces cerevisiae*. Nat. Prod. Res. 22, 414–421. <https://doi.org/10.1080/14786410701591622>.
- Srivastava, V., Nand, K.N., Ahmad, A., Kumar, R., 2023. Yeast-based virus-like particles as an emerging platform for vaccine development and delivery. Vaccines 11 (2), 479. <https://doi.org/10.3390/vaccines11020479>.
- Superti, F., Ammendolia, M.G., Tinari, A., Bucci, B., Giammarioli, A.M., Rainaldi, G., Rivabene, R., Donelli, G., 1996. Induction of apoptosis in HT-29 cells infected with SA-11 rotavirus. J. Med. Virol. 50, 325–334. [https://doi.org/10.1002/\(SICI\)1096-9071\(199612\)50:4<325::AID-JMV8>3.0.CO;2-A](https://doi.org/10.1002/(SICI)1096-9071(199612)50:4<325::AID-JMV8>3.0.CO;2-A).
- Taban, I.M., Zhu, J., Deluca, H.F., Simons, C., 2017. Analysis of the binding sites of vitamin D 1 $\alpha$ -hydroxylase (CYP27B1) and vitamin D 24-hydroxylase (CYP24A1) for the design of selective CYP24A1 inhibitors: Homology modelling, molecular dynamics simulations and identification of key binding requirements. Bioorg. Med. Chem. 25, 5629–5636. <https://doi.org/10.1016/j.bmc.2017.08.036>.
- Thomas, E.E., Puterman, M.L., Kawano, E., Curran, M., 1988. Evaluation of seven immunoassays for detection of rotavirus in pediatric stool samples. J. Clin. Microbiol. 26 (6), 1189–1193. <https://doi.org/10.1128/jcm.26.6.1189-1193.1988>.
- Tomas, M., Capanoglu, E., Bahrami, A., Hosseini, H., Akbari-Alavijeh, S., Shaddel, R., Jafari, S.M., 2022. The direct and indirect effects of bioactive compounds against coronavirus. Food Front. 3 (1), 96–123. <https://doi.org/10.1002/fft2.119>.
- Trojnar, E., Sachsenröder, J., Twardziok, S., Reetz, J., Otto, P.H., Johne, R., 2013. Identification of an avian group A rotavirus containing a novel VP4 gene with a close relationship to those of mammalian rotaviruses. J. Gen. Virol. 94 (1), 136–142. <https://doi.org/10.1099/vir.0.047381-0>.
- van Vuuren, S.F., 2008. Antimicrobial activity of South African medicinal plants. J Ethnopharmacol. 119 (3), 462–472. <https://doi.org/10.1016/j.jep.2008.05.038>.
- Vanachayangkul, P., Chow, N., Khan, S.R., Butterweck, V., 2011. Prevention of renal crystal deposition by an extract of *Ammi visnaga* L. and its constituents khellin and visnagin in hyperoxaluric rats. Urol. Res. 39, 189–195. <https://doi.org/10.1007/s00240-010-0333-y>.
- Varsha, K.K., Narisetty, V., Brar, K.K., Madhavan, A., Alphy, M.P., Sindhu, R., Binod, P., 2023. Bioactive metabolites in functional and fermented foods and their role as immunity booster and anti-viral innate mechanisms. J. Food Sci. Technol. 60 (9), 2309–2318. <https://doi.org/10.1007/s13197-022-05528-8>.
- WHO/FAO. (2002). Guidelines for the evaluation of probiotics in food. London: Food and Agriculture Organization of the United Nations and World Health Organization Working Group.
- Wollowski, I., Rechkemmer, G., Pool-Zobel, B.L., 2001. Protective role of probiotics and prebiotics in colon cancer. Am. J. Clin. Nutr. 73 (2), 451–455. <https://doi.org/10.1093/ajcn/73.2.451s>.
- World Health Organization (WHO), 2009. Manual of rotavirus detection and characterization methods. pp 149, publication is available on the [www.who.int/vaccines-documents](http://www.who.int/vaccines-documents) induced by a rotaviral nonstructural glycoprotein. Science 272, 101–104.
- World Health Organization (WHO), (2004): Guidelines for drinking-water quality. Geneva, Switzerland. 3<sup>rd</sup> ed, vol 1, p: 515.
- Yasumura, Y., Kawakita, Y., 1963. Studies on SV40 in tissue culture—preliminary step for cancer research “*in vitro*”. Nihon Rinsho 21, 1201–1215.
- Yonekura-Sakakibara, K., Higashi, Y., Nakabayashi, R., 2019. The origin and evolution of plant flavonoid metabolism. Front. Plant Sci. 10, 943. <https://doi.org/10.3389/fpls.2019.00943>.